Effect of process parameters on microstructural and mechanical properties of friction stir welded dissimilar aluminium alloys AA 6061 and AA 7075

R. Manikandan and G. Elatharasan*

Department of Mechanical Engineering,
University College of Engineering Pattukkottai,
Anna University,
Rajamadam – 614701, Tamilnadu, India
Email: rmkravi90@gmail.com
Email: gelatharasan@gmail.com
*Corresponding author

Abstract: Frictions stir welding of dissimilar alloys are an efficient way in industrial applications. The effect of joining dissimilar alloys (AA6061-AA7075) has improves the mechanical strength of the welded joint. This work investigated the micro-hardness and mechanical properties of frictions stir welded dissimilar alloys. Aluminium alloy is heat treatable and may be subjected to either hot working or cold working. The heat treatment is followed by revolutionising and precipitation hardening. Microhardness was measured at various zones of the welded joints. The tensile properties of dissimilar joints are characterised. Tensile test results distributed the material flow and the stress-strain curve designates the mechanical strength of the frictions stir welding parameters. Cylindrical threaded profile has an important role among the other tool profiles. It contributes 93% to the overall efficiency. The high strength of 172 MPa was attained in the tool which is made up of cylindrical threaded pin profiled tool. This work inferred that the rotational speed, transverse speed, and D/d ratio for cylindrical threaded are considered more efficient. Maximum tensile strength could be obtained from the cylindrical threaded tool and it is comparatively high than other materials. Tensile and hardness measurement were done on this part of material characterisation.

Keywords: friction stir welding; FSW; micro hardness; dissimilar alloys; aluminium; heat treatment; cylindrical.

Reference to this paper should be made as follows: Manikandan, R. and Elatharasan, G. (2020) 'Effect of process parameters on microstructural and mechanical properties of friction stir welded dissimilar aluminium alloys AA 6061 and AA 7075', *Int. J. Rapid Manufacturing*, Vol. 9, No. 1, pp.1–15.

Biographical notes: R. Manikandan was awarded with his Masters in CAD/CAM from the Anna University Tirunelveli during 2014. In August, he joined as an Assistant Professor at the University College of Engineering Pattukkottai in the Department of Mechanical Engineering. He has published in ten international journals, six international conferences and two national journals.

G. Elatharasan was awarded with a PhD in Friction Stir Welding from the Anna University Chennai. He is a member of faculty in the Anna University since 2001. He has published research papers in 34 international journals, 16 international conferences, and 15 national journals.

1 Introduction

Friction stir welding (FSW) is a solid-state fusion technique, which was invented by the Welding Institute (TWI), UK, in 1991 (Thomas et al., 1991). Aluminium alloys (AA6061-AA7075) are most widely used in a multiplicity of industrial applications: for making an aircraft structure and marine applications, automotive and shipbuilding, pipelines and storage tanks, etc. (He et al. 2012; He, 2010, 2012; Elatharasan and Senthil Kumar, 2013). There is an increasing design needs due to the lightweight structures of vehicle body shells. FSW technique is a unique approach for providing lightweight structures of dissimilar alloys (He et al., 2008). The technique defects of approximating porosity, slag, segregation, liquid cracking and heat affected zone (HAZ) could be avoided. Consequently, the dissimilar alloys of joint technology are a part of the manufacturing process since fusion welding of dissimilar alloys has melted with formation of secondary phase due to temperature absences with the help of base materials as a pin device (Sheikhi and Bolfarini, 2007; Xue et al., 2011; Buffa et al., 2006). As the temperature distribution have compared with the dissimilar alloys of both advanced side and retracting sides of nugget zones (NZs) has gradually increased for the corresponding high rotational speeds. The best parameters collected are rotational speed, and transverse speed. Hence, the tool provides a vital role in FSW (Padmanaban and Balasubramanian, 2009). This tool profile or shape in favour of cylindrical, squared, trigonal and threaded is efficient to transfer the material from base material by stirring action. The behaviour of FSW more than belong to the tool profile and different process parameters involved (Dinesh et al., 2018). The schematic diagram of a FSW is shown in Figure 1.

Figure 1 Friction stir welding

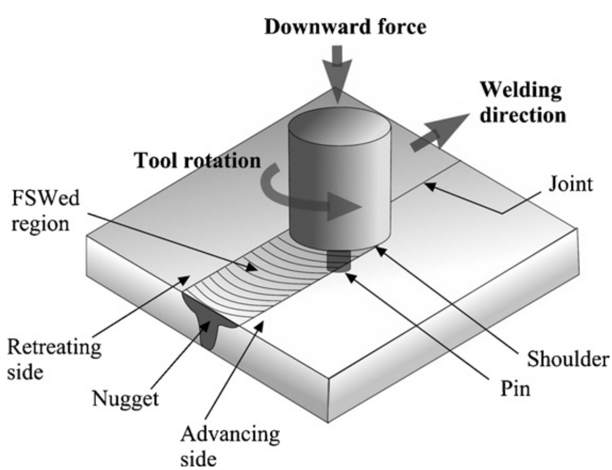

FSW has recognised the four functional areas such as parent material (PM), NZ, thermo mechanically affected zone (TMAZ), and HAZ with the help of optical electron microscope (He et al., 2014). These all the zones generate according to the material flow along the welding line. The heat generation of rubbing tool has enhanced the plastic deformation on work piece of top surface. At the same time, the ratio of swept volume to pin volume is known as material flow behaviour. The swirl rotates according to the rotational speed and transverse speed for the required condition (Thomas et al., 2003).

Earlier researches lot of investigation done by the aluminium alloys AA 6061 and AA 7075 in FSW. There are no more brief researches of microstructure in dissimilar FSW joint and mechanical properties studies (Elangovan et al., 2009). In this paper investigated the tensile and micro hardness test of the dissimilar alloys and FSW process parameter reviewed by the microstructure of the welded joint using optical microscope. The basics of this design concept in FSW to join dissimilar alloys completed from using different tool profiles, which has reported. Defects of different tool profile in AA 6061 have analysed and have experimented in Arora et al. (2010). However, effect of tool pin profiles with rotational speed generated the heat plastic behaviour on the plate surface. This information is very useful for FSW process. The hardness survey of the welding zone has investigated the effect of process parameter seeing that the macroscopic and microscopic structures. The correlation between the microstructure as well as mechanical properties was explained in detail.

2 Tool design

Tool design is an integrated part of FSW process. It evaluates the material flow characterisation for both types of aluminium wrought alloys (Francis et al., 2014). This welding tool should contain height, depth, pin and shoulder, respectively. Pin and shoulder are the two main features of FSW process. This FSW types of pin shapes such as straight cylindrical, threaded cylindrical, taper threaded, squared shapes has investigated. The rotating pins to mixed the materials as the advancing side and retracting sides. This pin will cause a material deformation to the purpose of joined the materials. Various types of tool were used to investigate the mechanical properties and material flow characterisation (Rai et al., 2011). The tool different shapes, temperature distributed as a heat transfer mechanics to mixing the material during the FSW process at the maximum temperature of dissimilar alloys. The power send through a tool, it was rotate and enhanced with material flow behaviours. The principle of tool criterion some amount of torque applied at end of the pin. The torque proposed as traction forces could be tested (Arora et al., 2011). The optimum parameters of a tool shoulder with heat transfer and material flow behaviours it among the weld material the temperature commonly lived with particular range. Effect of tool shoulder was investigated as a flow model (Mehta et al., 2011; Elatharasan and Senthil Kumar, 2012). This thermocouple used to observed were investigated a temperature distribution and material deformation in FSW process (Zhang et al., 2009; Zhang and Liu, 2011). The FSW zones of grain sizes can be controlled by the various tool sizes. These tool end surfaces having different shapes as knurling, squared, threaded, scrolls, ridges as showed in Figure 2.

The tool pin surfaces should consist of certain features, as material flow behaviour and withstand good mechanical strength for the different loading conditions. The shoulder and work piece between high shear formation and deformation could be able to showing the material uniform mixing of the dissimilar alloys. The depth of the material deformed mainly governed by the probe area. This is necessary for to maintain the material flow behaviour and enabled the different tool pin performance. It provides a compressive force between the weld centre lines. The material convexity process promoted a NZs or placing stirring action. The probe of surface mainly used to resist the high force during the plunging. This material movement around the probe extremely complex and much different tool with each other.

Figure 2 Different tool profiles, (a) straight cylindrical (b) threaded cylindrical (c) tapered cylindrical (d) square (e) triangle

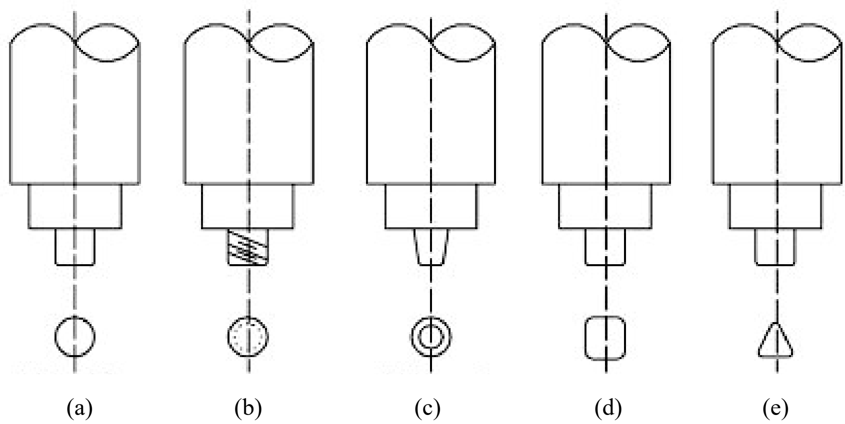

3 Experimental setup

FSW of an experimental setup has shows in Figure 3 (He, 2012; Elatharasan and Senthil Kumar, 2012). In this work investigated the dissimilar alloys AA 6061, magnesium and silicon. AA 6061 advanced side and other one AA 7075 acting as a retracting side (Elatharasan and Senthil Kumar, 2014). Because these AA 6061 alloys have high material flow stability and high resistance capability compared with other materials. Both the plates (100 × 100 × 6) have been used for this FSW process. Chemical and mechanical properties of AA 6061 alloy properties are evaluated in Table 1. The trail experiments has conducted for joining of dissimilar alloys of various optimum limits such as rotational speed, transverse speed , and various load conditions. The FSW process is carried out by the vertical milling machine. These functions of process limits were constant for the different pin profiles. The dimension has considered 6mm thickness both plates and pin diameter 6mm, shoulder diameter 18 mm and height of the tool pin 5.5 mm. This tool pin has high thermal conductivity and high resistance (Dinesh et al., 2016; Heidarzadeh et al., 2012; Jayaraman et al., 2009; Desai et al., 2017). The tool pin is placed on the centre of the welded plate. A total of nine samples were tested with different process parameters such as rotational speed, transverse speed and loading conditions. The welding condition and process parameters are shown in Table 3 (Srivastava et al., 2018).

Figure 3 Location of tensile assessment specimens in the FS welded joints

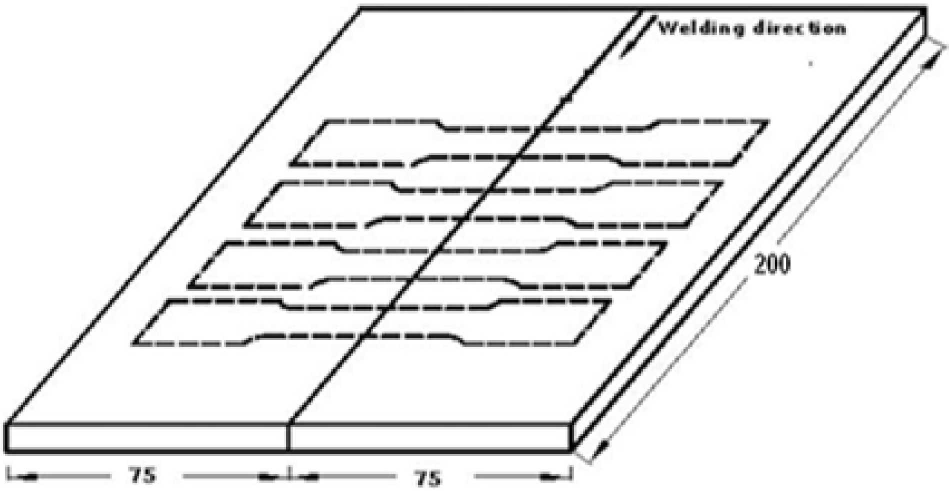

Table 1 Chemical composition of dissimilar alloys

Element	*Mg*	*Mn*	*Zn*	*Fe*	*Cu*	*Si*	*Cr*	*Al*
AA6061-T6	0.84	0.01	0.06	0.40	0.24	0.54	0.18	bal
AA7075-T6	2.1	0.12	5.1	0.35	1.2	0.58	1.2	bal

Table 2 Mechanical properties of dissimilar alloys

Element	*Yield strength (MPa)*	*Tensile strength (MPa)*	*Elongation (%)*
AA6061-T6	306	342	17
AA7075-T6	469	578	11

Table 3 FSW parameters

S. no.		*Rotational speed (rpm)*	*Translational speed (mm/min)*	*Pin profile*
1	*Welding parameters*	800	30	cylindrical
2		1,000	60	Threaded cylindrical
3		1,200	90	Taper threaded

Tensile test was carried out by the UTM machine. The hardening of precipitated dissimilar alloys as a welded work pieces carried out for certain amount of load acting on the transverse direction. Tensile test were nine samples has prepared and optimum values of average value taken into account.

Vickers hardness (Wilson Wolpert – Germany) test has done on the nugget region as a transverse load section of Welded zones. This area considered as a TMAZ. The hardness of variation region as different tool profiles has investigated or plotted for the following sections. The various regions of TMAZ zones determined by the microstructure of the both dissimilar alloys. Nevertheless, the fluctuation between the various regions has measured from the hardness values.

4 Result and discussions

4.1 Tensile test

The tensile samples extracted from the welded plates shows that figure. Tensile test methods are processed according to the design rules in the ASTM standards. Three different pin profiles were used for the welded joints, to make sure the repeatability of welding consistency and testing are carried out. The calculated test readings and plotted graphs are shown. The welded region observation of the graph of welded work pieces are good mechanical properties with on three different profile cases. And Figure 5 shows after tensile nature of the material and demonstrating the fractured areas. The fractured area for the effect of tool pin profiles of NZs has tested.

Figure 4 Before tensile test (see online version for colours)

Figure 5 After tensile test (see online version for colours)

The tensile properties of joint welded pieces of precipitation hardening will increase with the base material, consisting of mechanical properties and tensile behaviour, characterised by the thermal history. It affects the grain boundaries due to some precipitation hardening dissolution of affecting tensile properties of the joints. From above, all the joints of nine samples have low ductility to make sure of the strength of the dissimilar alloys.

Figure 6 Tensile test, (a) cylindrical tool profile (b) cylindrical threaded tool profile (c) taper tool profile (see online version for colours)

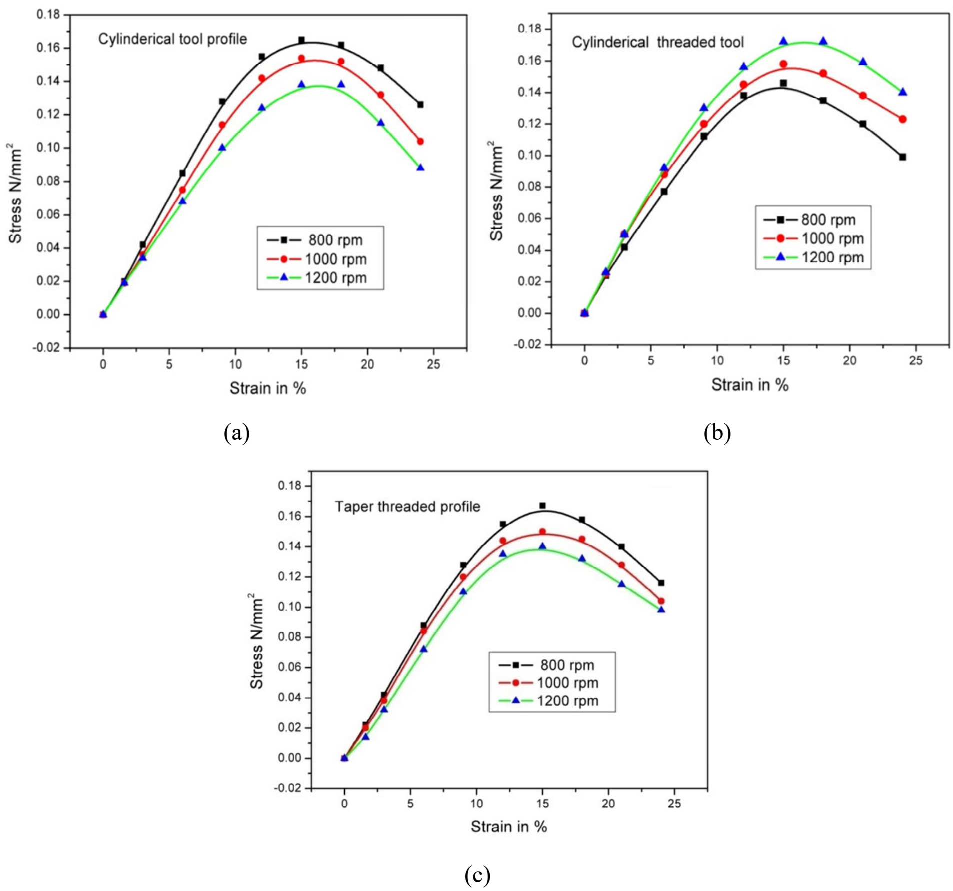

Figure 7 Dimensions of the tensile specimen (ASTM E8M-04)

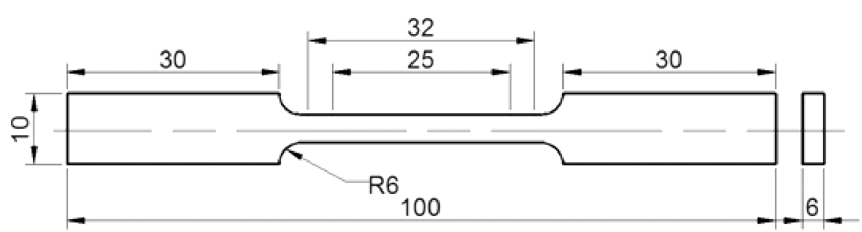

Figure 7 showing dimension of the specimen. The optimised parameters obtained like rotational speed, transverse speed and D/d ratios are 1,200 rpm, 60 mm/min, and 6. Cylindrical threaded profile obtained the optimum value compared to other profiles. It contributes 93% to the overall efficiency. The highest strength 172 Mpa obtained by the cylindrical threaded tool. The effect of tensile behaviour of welded joints is evaluated. The welded joints are lower strength than other PMs.

And the stirred zone or NZs are to indented the fracture behaviour occur compared with zones. Since the fracture at a maximum stress state to showed the ductility of the materials. The fracture also occurred at TMAZ of AA 6061 and AA 7075.

4.2 Hardness measurements

The micro hardness value corresponding to the different combinations of welding speed, Transverse speed and axial loads as showed in below the graph. The NZs of hardness values obtained the good bonded strength and high hardness value. These values are shows a decreasing from end of the beginning as advancing side (AA 6061) and retracting side (AA 7075) has gradually increased. It is also noted that from the graph values to find the different zones performing to increase the weld ability of the dissimilar structures. Along these values of TMAZ zones has advanced side (AA 6061) higher than that of retracting side (AA 7075) (minimum hardness zone). It will be denoted by a NZ that illustrated a fracture of the tensile specimen. This nature of welding direction of stirred zone to expressed as a fine grain sizes of the dissimilar alloys. It is an important role for the nature of mixture the material corresponding diffusion as AA 6061 materials. The optimum parameters, transverse speed 60 mm/min gradually; rotational speed 1,000 rpm value was found to increase the hardness value 92 HV obtained for the taper threaded tool profile. Further increasing rotational speed and decrease hardness value as for the same tool profile. At constant speed will increase 1,200 rpm, the hardness value also decreased. The welding region, found the maximum hardness value and average values calculated for the each sample. The appearance of NZ with the centre line to causes very efficiently. Almost hardness value increased gradually in HAZ. This fracture takes place on the NZs and relative to another. The advancing side takes more hardness values comparatively; lower value obtained the retracting sides. These higher hardness values found in the cylindrical tool profile. NZs are seems higher value compared with the TMAZ zones. While hardness values are proportional to the tensile values. The taper threaded profile obtained higher hardness value.

Figure 8 Vickers hardness value for cylindrical tool (see online version for colours)

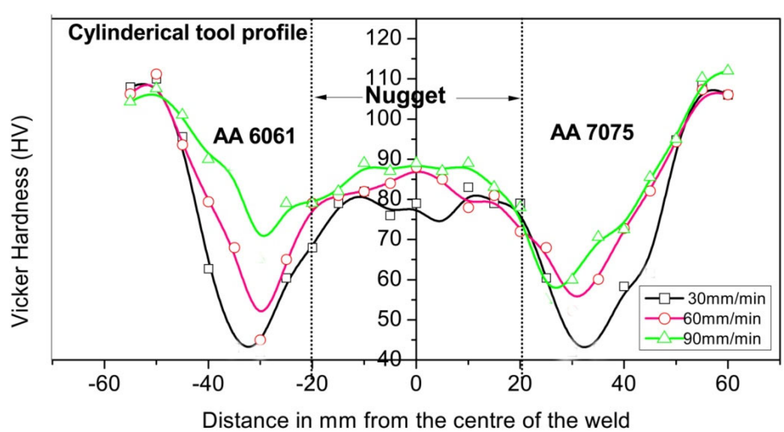

Figure 9 Vickers hardness value for cylindrical threaded tool (see online version for colours)

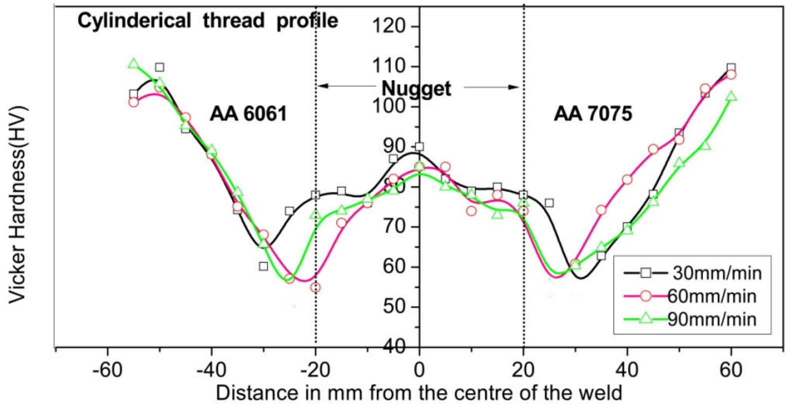

Figure 10 Vickers hardness value for taper tool (see online version for colours)

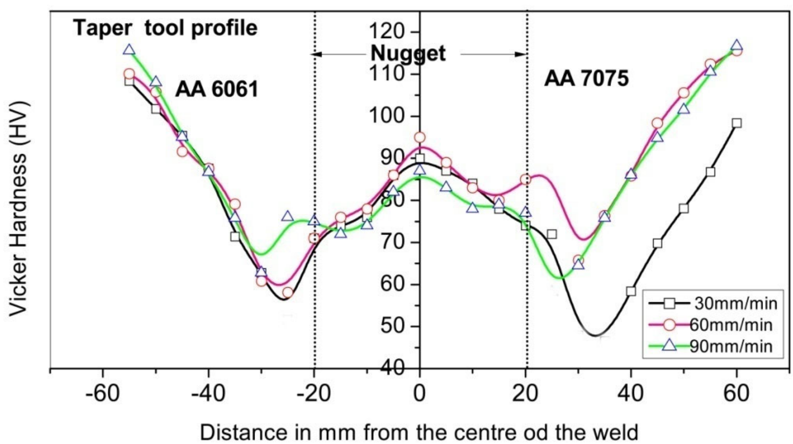

4.2.1 Nugget zones

The hardness value fluctuated between the tools as shows in the above graphical image. This NZ and thermo-mechanically affected zone, mixing the both materials under the different process parameters of the welded joint. The effectiveness of different optimum limits the material flow in NZ and other eutectic zones has showed to the effects of a tool profiles. The detailed about NZ distribution was studied in Zhang and Zhang (2006). Some insufficient loading condition test pieces to specify down the failures. The axial load performance has discussed in Zhang et al. (2007). Crystallisation effect is an important role in this FSW process. It contributes decreasing the hardness of the base material from its centre line and rotational speed to control the high degree softening weld NZs. And it all the hardening and softening precipitations has shown in Figures 11, 12, 13, and 14.

Figure 11 Cylindrical, (a) parent AA 6061 (b) HAZ (c) macroscopic structure (d) NZ (e) TMAZ zone (see online version for colours)

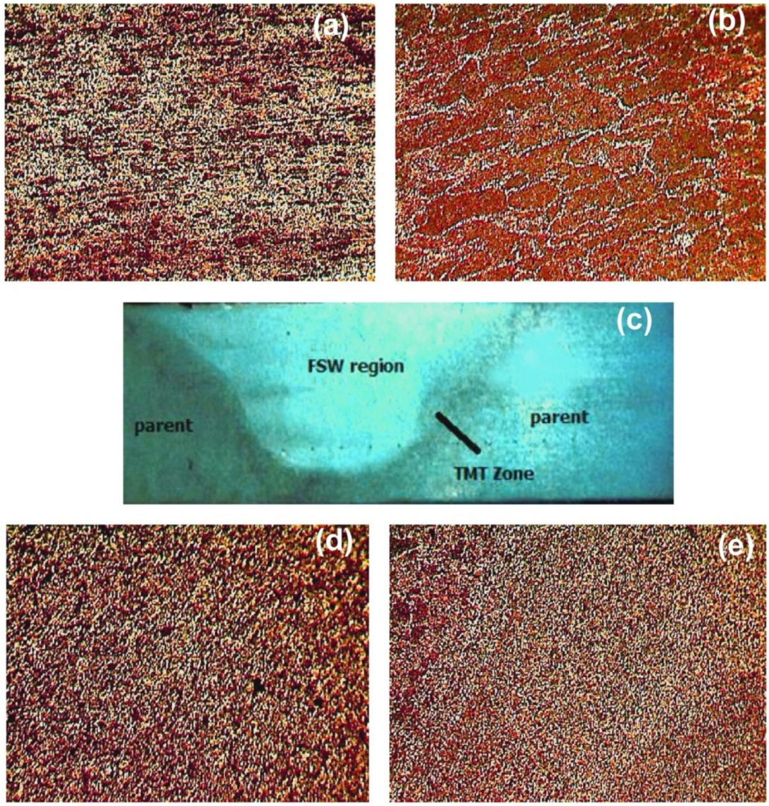

Figure 12 Macrostructure of heat zones in FSW (see online version for colours)

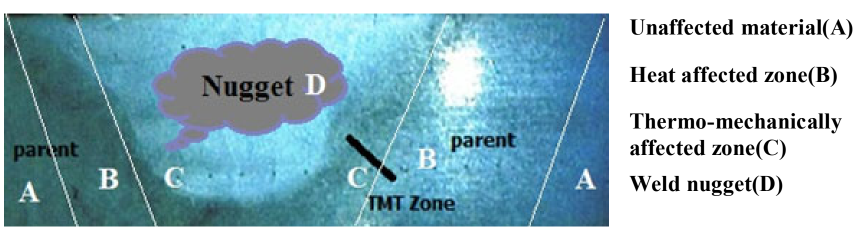

4.2.2 TMAZ zones

Thermo-Mechanically affected zone, it related to the of NZs. The relationship of welding zones has been investigated in the FSW process. Heat response is created to the centre line weld of both alloys carry work-hardening condition strongly to affect the structures, and controlled by the grain sizes. High temperature and mechanical pressure mixed with the both of the dissimilar alloys to joined with the of structure to achieved the strength of the superior weld. It can be some characterised on the boundary of NZs as both of the dissimilar alloys.

Figure 13 Cylindrical thread, (a) parent AA 6061 (b) HAZ (c) macroscopic structure (d) NZ (e) TMAZ zone (see online version for colours)

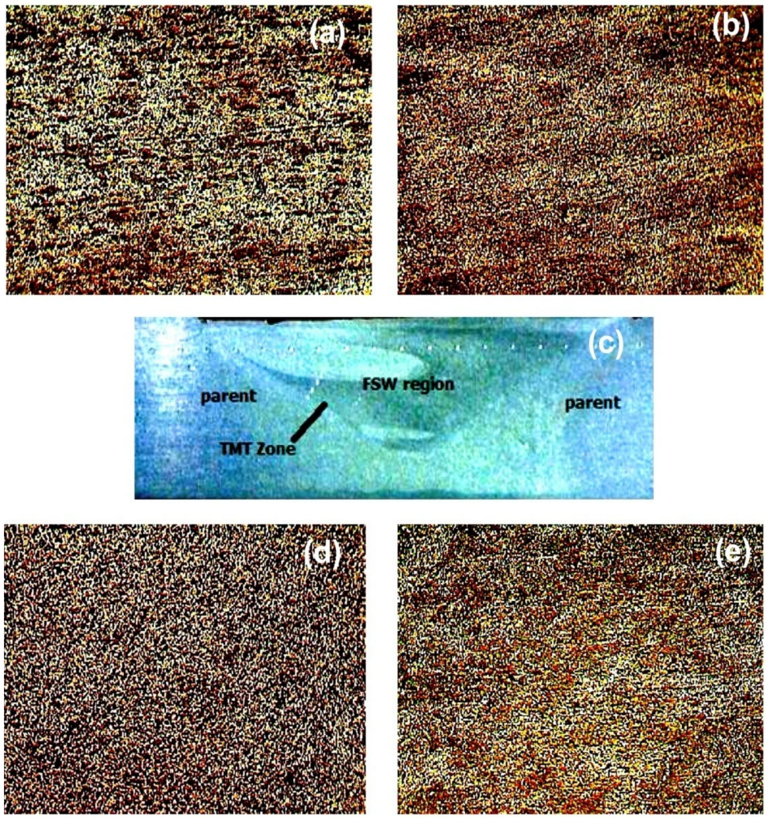

Figure 11 shows the parent metal of AA 6061 microstructure. The microstructure is fine precipitated particles of the eutectics of Mg2Si with some undissolved particles of intermetallic namely (FeMn) Al6. The particles of strengthening are fine and uniformly distributed adding higher hardness to the metal matrix. HAZ place which is very close to the NZ. The heat of the process made the grain to grow and changed the grain flow direction. In this NZ on the surface have been added both heat and the mechanical forces, acted. The heating and the later cooling of the process made the eutectics to re-appear from the aluminium solid solution and fragmented due to the stirring action of the pin of the nugget tool. This zone shows the user interface zone of the both TMT zone and the nugget. While the NZ shows the fine particles of the eutectics, the TMT zone shows the larger particles which have not come in contact with the tool but its direction changed due to the plastic flow.

Figure 13 shows the parent metal AA6061 microstructure. The microstructure is fine precipitated particles of the eutectics of Mg2Si with some undissolved particles of intermetallic namely (FeMn) Al6. The particles of strengthening are fine and uniformly distributed adding higher hardness to the metal matrix. Shoulder zone of the specimen which has subjected to FSW. The zone is the advancing side of the specimen with grain flow due to the mechanical forces and the heat due to friction. The heating and the later cooling of the process made the eutectics to re-appear from the aluminium solid solution and fragmented due to the stirring action of the pin of the nugget tool. The HAZ of at the vicinity of the FSW zone clearly observed. The particles of the eutectics are more and bigger.

Figure 14 Taper threaded, (a) parent AA 6061 (b) HAZ (c) macroscopic structure (d) NZ (e) TMAZ zone (see online version for colours)

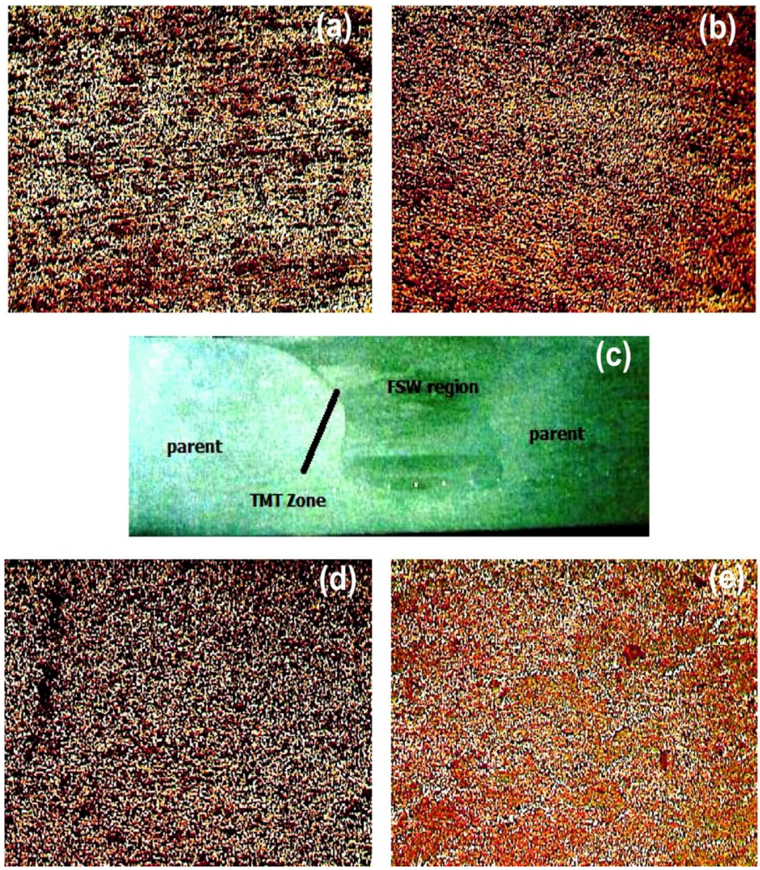

Figure 14 shows the parent metal AA 6061 microstructure. The microstructure is fine precipitated particles of the eutectics of Mg2Si with some dissolved particles of intermetallic namely (FeMn) Al6. The particles of strengthening are fine and uniformly distributed adding higher hardness to the metal matrix. The HAZ where the direction has changed but the grains remains small. HAZ where the particles of the eutectics have become bigger due to growth but in the same direction as that of the parent metal direction. The heating and the later cooling of the process made the eutectics to re-appear from the aluminium solid solution and fragmented due to the stirring action of the pin of the nugget tool.

4.2.3 Macrostructure

The macrostructure observation discovered the different HAZs for the both PM. Figures 11, 12, 13, and 14 display the appearance of the FSW zones. Figure 11 demonstrates the uniform distribution of the plastic flow behaviour like an elliptical shape of the dissimilar alloys. And Figure 12 indicates the NZ, TMAZ, HAZ than PM. Sufficient heat generation to avoiding the tunnel defect (Figures 13 and 14), warming and piping defects. The macrostructure obviously to create a defect free weld for the appropriate heat generation.

5 Conclusions

FSW of dissimilar alloys are achieved the good weld ability and performance characteristics. Were investigated the tool profile, microstructure and tensile properties of dissimilar alloys AA 6061 and AA 7075. This work inferred that the rotational speed transverse speed, and D/d ratio for cylindrical threaded profile pin considered as more efficient. Maximum tensile strength obtained from the cylindrical threaded tool and it has comparatively high as other than materials. Cylindrical threaded profile roles better to among the other tool profiles. The fabricated joint using cylindrical threaded tool and the tool rotational speed 1,200 rpm and transverse speed 60 mm/min and yielded highest strength of 172 Mpa. The taper threaded cylindrical profile has value 92 HV obtained. This tool behaviour created a bonding with both of the dissimilar alloys (AA6061 and AA7075). Using Vickers hardness (Wilson Wolpert – Germany) microstructural studies to established the better structures of dissimilar alloy. The influences of Keller Reagent used to polish the more number of times and to get the FSW of functional working zones. It adopt with the better mechanical properties and microstructures characterisation. The welding consistency purpose of the test conducted, and repeated times at different optimisation parameters. The cylindrical threaded tool profile has obtained best strength among the other two pin profiles.

References

Arora, A., De, A. and Debroy, T. (2011) 'Toward optimum friction stir welding tool shoulder diameter', *Scripta Materialia*, Vol. 64, No. 1, pp.9–12.

Buffa, G.J., Huaa, R., Shivpuri, A. and Fratini, L. (2006) 'Design of friction stir welding tool using the continuum based FE model', *Materials Science and Engineering A*, Vol. 485, pp.367–374.

Desai, B.V. Desai, K.P. and Raval, H.K. (2017) 'The performance of tool shape on efficiency and quality of forming in incremental sheet-forming process', *International Journal of Rapid Manufacturing (IJRAPIDM)*, Vol. 6, No. 4, pp.215–234.

Dinesh, S., Godwin, A.A., Rajaguru, K. and Vijayan, V. (2016) 'Investigation and prediction of material removal rate and surface roughness in CNC turning of En24 alloy steel', *Mechanics and Mechanical Engineering*, Vol. 20, No. 4, pp.451–466.

Dinesh, S., Godwin Antony, A., Rajaguru, K. and Vijayan, V. (2018) 'Comprehensive analysis of wire electric discharge machining process in machining high chromium high carbon steel', *International Journal of Mechanical and Production Engineering Research and Development*, February, Vol. 8, No 1, pp.65–74.

Dinesh, S., Godwin, A.A., Rajaguru, K. and Vijayan, V. (2016) 'Experimental investigation and optimization of machining parameters in CNC turning operation of duplex stainless steel', *Asian Journal of Research in Social Sciences and Humanities*, October, Vol. 6, No. 10, pp.179–195.

Elangovan, K., Balasubramanian, V. and Valliappan, M. (2009) 'Effect of welding speed and tool pin profile on tensile properties of friction stir welded AA6061 aluminium alloy', *Int. J. of Microstructure and Materials Properties*, Vol. 4, No. 4, pp.455–475.

Elatharasan, G. and Senthil Kumar, V.S. (2013) 'An experimental analysis and optimization of process parameter on friction stir welding of AA 6061-T6 aluminum alloy using RSM', *International Conference on Design and Manufacturing*, *IConDM*, Vol. 64, pp.1227–1234.

Elatharasan, G. and Senthil Kumar, V.S. (2012) Modeling and optimization of friction stir welding parameters for dissimilar alloys using RSM', *Proceedings of the International Conference on Modeling and Optimization Computing*, Vol. 38, pp.3477–3481.

Elatharasan, G. and Senthil Kumar, V.S. (2014) 'Corrosion analysis of friction stir-welded AA 7075 aluminium alloy', *Journal of Mechanical Engineering*, Vol. 60, No. 1, pp.29–34.

Francis, J., Sparks, T.E., Ruan, J. and Liou, F. (2014) 'Multi-axis tool path generation for surface finish machining of a rapid manufacturing process', *International Journal of Rapid Manufacturing (IJRAPIDM)*, Vol. 4, No. 1, pp.66–80.

He, X., Gu, F. and Ball, A. (2012) 'Recent development in finite element analysis of self-piercing riveted joints', *Int. J. Adv. Manuf. Technol.*, Vol. 58, pp.643–649.

He, X. (2012) 'Finite element analysis of laser welding: a state of art review', *Mater. Manuf. Process*, Vol. 27, No. 12, pp.1354–1365.

He, X. (2010) 'Recent development in finite element analysis of clinched joints', *Int. J. Adv. Manuf. Technol.*, Vol. 48, pp.607–612.

He, X., Pearson, I. and Young, K. (2008) 'Self-pierce riveting for sheet materials: state of the art', *J. Mater. Process. Technol.*, Vol. 199, pp.27–36.

He, X., Gu, F. and Ball, A. (2014) 'A review of numerical analysis of friction stir welding', *Material Science and Engineering*, Vol. 65, No. 1, pp.651–666.

Heidarzadeh, A., Khodaverdizadeh, H., Mahmoudi, A., Nazari, E. (2012) 'Tensile behavior of friction stir welded AA 6061-T4 aluminum alloy joints', *Materials and Design*, Vol. 37, pp.166–173.

Jayaraman, M., Sivasubramanian, R., Balasubramanian, V. and Lakshminarayanan, A.K. (2009) 'Application of RSM and ANN to predict the tensile strength of friction stir welded A319 cast aluminium alloy', *Int. J. of Manufacturing Research*, Vol. 4, No. 3, pp.306–323.

Mehta, M., Arora, A., De, A. and Debroy, T. (2011) 'Tool geometry for friction stir welding – optimum shoulder diameter', *Metall MaterTrans A*, Vol. 42, No. 9, pp.2716–2722.

Padmanaban, G. and Balasubramanian, V. (2009) 'Selection of FSW tool in profile, shoulder and material for joining AZ31B magnesium alloy – an experimental approach', *Material and design*, Vol. 30, No. 7, pp.2647–2656.

Rai, R., De, A., Bhadeshia, H.K.D.H. and Debroy, T. (2011) 'Review friction stir welding join', *Science and Technology of Welding and Joining*, Vol. 16, No. 4, pp.325–342.

Sheikhi, S. and Bolfarini, C. (2007) 'Preliminary study on the microstructure and mechanical properties of dissimilar friction stir welding in aircraft aluminium alloys 2024-T351 and 6065-T4', *Journal of Materials Processing Technology*, Vol. 6, No. 4, pp.132–142.

Srivastava, M., Rathee, S., Maheshwari, S. and Kundra, T.K. (2018) 'Multi-objective optimization of fused deposition modelling process parameters using RSM and fuzzy logic for build time and support material', *Int. J. of Rapid Manufacturing*, Vol. 7, No. 1, pp.25–42.

Thomas, W.M., Dolby, R.E., David, S.A., DebRoy, T., Lippoid, J.C. and Smart, H.B. (2003) *In Processing of the Sixth International Conference on Trenda in Welding Research Pine Mountain*, ASM International, GA, pp.203–211.

Xue, P., Ni, D.R., Wang, D., Xiao, B.L. and Ma, Z.Y. (2011) 'Effect of friction stir welding parameters on the microstructure and mechanical of dissimilar alloys Al-Cu joints', *Materials Science and Engineering A*, Vol. 528, No. 1, pp.13–14.

Zhang, Z., Liu, Y.L. and Chen, J.T. (2009) 'Effect of shoulder size on the temperature rise and the material deformation in friction stir welding', *Int. J. Adv. Manuf. Technol.*, Vol. 45, No. 1, pp.889–895.

Zhang, Z. and Liu, H.J. (2011) 'Effect of pin shapes on material deformation and temperature field in friction stir welding', *Trans Chin. Weld. Inst.*, Vol. 32, pp.5–8.

Zhang, Z. and Zhang, H.W. (2006) 'Numerical simulation of dynamic recrystallization and hardness distribution in friction stir welding process', *Acta Metall Sinica*, Vol. 42, No. 9, pp.998–1002.

Zhang, Z., Liu, Y.L. and Zhang, H.W. (2007) 'Effect of variation of axial load on material deformations and temperature distributions in friction stir welding', *Acta Metall Sinica*, Vol. 43, No. 8, pp.868–874, in Chinese.